European Heart Journal (2017) **38**, 362–372
doi:10.1093/eurheartj/ehw333

BASIC SCIENCE

Iron-regulatory proteins secure iron availability in cardiomyocytes to prevent heart failure

Saba Haddad[1,2], Yong Wang[1,2], Bruno Galy[3,4], Mortimer Korf-Klingebiel[1,2], Valentin Hirsch[1,2], Abdul M. Baru[1,2], Fatemeh Rostami[1,2], Marc R. Reboll[1,2], Jörg Heineke[2], Ulrich Flögel[5], Stephanie Groos[6], André Renner[7], Karl Toischer[8], Fabian Zimmermann[9], Stefan Engeli[10], Jens Jordan[10], Johann Bauersachs[2], Matthias W. Hentze[3], Kai C. Wollert[1,2], and Tibor Kempf[1,2]*

[1]Division of Molecular and Translational Cardiology, Hannover Medical School, Carl-Neuberg-Straße 1, 30625 Hannover, Germany; [2]Department of Cardiology and Angiology, Hannover Medical School, Carl-Neuberg-Straße 1, 30625 Hannover, Germany; [3]European Molecular Biology Laboratory, Meyerhofstraße 1, 69117 Heidelberg, Germany; [4]Division of Virus-associated Carcinogenesis, German Cancer Research Centre, Im Neuenheimer Feld 280, 69120 Heidelberg, Germany; [5]Department of Molecular Cardiology, University of Düsseldorf, Universitätsstraße 1, 40225 Düsseldorf, Germany; [6]Institute of Cell Biology, Hannover Medical School, Carl-Neuberg-Straße 1, 30625 Hannover, Germany; [7]Department of Thoracic and Cardiovascular Surgery, University of Bochum, Georgstraße 11, 32545 Bad Oeynhausen, Germany; [8]Department of Cardiology and Pneumology, University of Göttingen, Robert-Koch-Straße 40, 37075 Göttingen, Germany; [9]Department of Analytical Chemistry, Leibniz University Hannover, Callinstraße 1, 30167 Hannover, Germany; and [10]Institute of Clinical Pharmacology, Hannover Medical School, Carl-Neuberg-Straße 1, 30625 Hannover, Germany

Received 30 November 2015; revised 27 June 2016; accepted 12 July 2016; online publish-ahead-of-print 21 August 2016

See page 373 for the editorial comment on this article (doi: 10.1093/eurheartj/ehw386)

Aims Iron deficiency (ID) is associated with adverse outcomes in heart failure (HF) but the underlying mechanisms are incompletely understood. Intracellular iron availability is secured by two mRNA-binding iron-regulatory proteins (IRPs), IRP1 and IRP2. We generated mice with a cardiomyocyte-targeted deletion of Irp1 and Irp2 to explore the functional implications of ID in the heart independent of systemic ID and anaemia.

Methods and results Iron content in cardiomyocytes was reduced in Irp-targeted mice. The animals were not anaemic and did not show a phenotype under baseline conditions. Irp-targeted mice, however, were unable to increase left ventricular (LV) systolic function in response to an acute dobutamine challenge. After myocardial infarction, Irp-targeted mice developed more severe LV dysfunction with increased HF mortality. Mechanistically, the activity of the iron–sulphur cluster-containing complex I of the mitochondrial electron transport chain was reduced in left ventricles from Irp-targeted mice. As demonstrated by extracellular flux analysis *in vitro*, mitochondrial respiration was preserved at baseline but failed to increase in response to dobutamine in Irp-targeted cardiomyocytes. As shown by ^{31}P-magnetic resonance spectroscopy *in vivo*, LV phosphocreatine/ATP ratio declined during dobutamine stress in Irp-targeted mice but remained stable in control mice. Intravenous injection of ferric carboxymaltose replenished cardiac iron stores, restored mitochondrial respiratory capacity and inotropic reserve, and attenuated adverse remodelling after myocardial infarction in Irp-targeted mice but not in control mice. As shown by electrophoretic mobility shift assays, IRP activity was significantly reduced in LV tissue samples from patients with advanced HF and reduced LV tissue iron content.

Conclusions ID in cardiomyocytes impairs mitochondrial respiration and adaptation to acute and chronic increases in workload. Iron supplementation restores cardiac energy reserve and function in iron-deficient hearts.

Keywords Iron deficiency • Heart failure • Energy metabolism • Extracellular flux analysis • ^{31}P-Magnetic resonance spectroscopy

*Corresponding author: Tel: +49 (0)511 532-2229, Fax: +49 (0)511 532-3357, Email: kempf.tibor@mh-hannover.de

Translational perspective

Iron deficiency (ID) is associated with adverse outcomes in heart failure, but the underlying mechanisms are incompletely understood. Here, we define the functional implications of ID in the heart independent of systemic ID and anaemia. We show that iron availability in cardiomyocytes is controlled by two mRNA-binding iron-regulatory proteins (IRPs). We find that IRP activity is reduced in the failing human heart and that selective IRP inactivation in mice promotes ID and mitochondrial dysfunction in cardiomyocytes. Iron deficiency in cardiomyocytes impairs, whereas iron supplementation restores the ability of the heart to adapt to acute and chronic increases in workload. These data provide strong mechanistic support for iron replacement therapies in patients with heart failure and ID.

Introduction

Iron deficiency (ID) is a frequent comorbidity in heart failure (HF).[1] Based on serum markers of depleted body iron stores, reduced systemic iron availability, and unmet cellular iron requirements, ~40% of patients with chronic HF and up to 75% of patients with acute (decompensated) HF are iron deficient.[2–4] Iron deficiency is more prevalent in HF patients with anaemia, but some patients are iron deficient and not anaemic.[2–4] At the tissue level, iron content in the myocardium is reduced by ~20–30% in patients with advanced HF.[5,6]

Iron is required for proper functioning of all mammalian cell types. Iron is a cofactor in haem and iron–sulphur cluster-containing proteins that control fundamental processes including oxygen transport (haemoglobin) and storage (myoglobin) and energy metabolism (e.g. components of the mitochondrial electron transport chain). Mitochondria are particularly abundant in the myocardium where they support the high energy demands of muscle contraction. Because small changes in cardiac energy metabolism can have a significan/t impact on contractile function, the heart may be particularly vulnerable to ID.[7]

Iron deficiency is associated with higher mortality rates in patients with acute or chronic HF independent of coexisting anaemia.[2–4] Iron supplementation improves symptoms and exercise capacity and may reduce the number of HF hospitalizations in iron-deficient patients with chronic HF.[8,9] Thus, it has been proposed that ID per se may contribute to adverse outcomes in HF, but mechanistic data supporting this hypothesis are lacking. Rats with severe nutritional ID develop anaemia and cardiac hypertrophy and may progress to overt HF.[10–12] However, these studies could not decipher the relative importance of anaemia leading to high-output HF and ID in the heart and in other non-haematopoietic tissues.

Intracellular iron availability is secured by two orthologous iron-regulatory proteins (IRPs), IRP1 and IRP2.[13] In iron-deficient cells, IRPs interact with conserved cis-regulatory iron-responsive elements (IREs) in the 5′ or 3′ untranslated regions of target mRNAs. Iron-regulatory protein binding to IREs increases the stability of transferrin receptor (iron import) mRNA and inhibits the translation of ferroportin (iron export) and ferritin H- and L-chain (iron sequestration) mRNAs. Iron-regulatory proteins thereby promote an increase in intracellular iron that is freely available for synthesis of haem and iron–sulphur cluster-containing proteins in the mitochondria or cytosol. When intracellular iron is high, IRP1 acquires an iron–sulphur cluster and loses its IRE binding capacity, whereas IRP2 is targeted for proteasomal degradation.[13]

Here, we show that IRP activity is diminished in the failing human heart, along with decreases in transferrin receptor expression and tissue iron concentration. To explore the functional implications, we generated mice with cardiomyocyte-selective deletion of Irp1 and Irp2. Irp-targeted mice developed ID specifically in the myocardium and enabled us to explore the role of cardiac ID without the confounding influence of systemic ID and anaemia.

Methods

Please refer to the Supplementary material online for an extended Methods section.

We collected left ventricular (LV) tissue samples from patients undergoing heart transplantation for ischemic or dilated cardiomyopathy and from unused donor hearts. The Ethics Committee of the University Hospital in Göttingen approved the study. All patients or their legal representatives provided written informed consent. Mice homozygous for floxed *Irp1* and floxed *Irp2* (Irp1/2$^{f/f}$) were bred to transgenic mice expressing Cre recombinase under the control of the β-myosin heavy chain promoter to generate mice with cardiomyocyte-targeted deletion of both *Irp1* and *Irp2* (Cre-Irp1/2$^{f/f}$). Irp1/2$^{f/f}$ littermates served as controls. Wild-type mice and Cre recombinase transgenic mice (Cre) were studied as well. Left ventricular pressure–volume loops were recorded with a 1.4F micromanometer-tipped conductance catheter inserted via the right carotid artery. The right jugular vein was canulated for dobutamine infusions. Myocardial infarction (MI) was induced by left anterior descending artery ligation. Two-dimensional transthoracic echocardiography was performed with a linear 30 MHz transducer. Oxygen consumption rate (OCR) and extracellular acidification rate (ECAR) were measured in isolated adult mouse cardiomyocytes with an XF^{e}24 analyser (Seahorse Bioscience). Cardiac high energy phosphates were monitored by acquisition-weighted two-dimensional ^{31}P chemical shift imaging at rest and during dobutamine infusion. Our local state authorities approved all animal procedures. Data are presented as mean ± SD. A two-tailed P value < 0.05 was considered to indicate statistical significance. The overall experimental design is summarized in Supplementary material online, *Figure S1*.

Results

Reduced iron content, IRE binding activity, and transferrin receptor expression in the failing human heart

Consistent with previous reports,[5,6] iron concentration was significantly lower in LV tissue samples from patients with advanced heart

failure than in LV tissue samples from unused donor hearts (*Figure 1A*). As shown by electrophoretic mobility shift assays, IRE binding activity was significantly reduced in failing hearts (most pronounced in patients with ischemic cardiomyopathy) (*Figure 1B*). Protein expression levels of the transferrin receptor were significantly lower in failing hearts than in the controls (*Figure 1C*).

Targeted Irp deletion in mice induces ID in the myocardium

We generated mice with a cardiomyocyte-targeted deletion of *Irp1* and *Irp2* (Cre-Irp1/2$^{f/f}$) to address Irp function in the heart (*Figure 2A*). Cre-Irp1/2$^{f/f}$ mice were born at the expected Mendelian inheritance ratio and survived into adulthood. Reverse transcriptase polymerase chain reaction on LV myocardium and isolated cardiomyocytes demonstrated near-complete Cre-mediated deletion of Irp1 and Irp2 mRNAs in cardiomyocytes from Cre-Irp1/2$^{f/f}$ mice compared with littermates lacking the Cre transgene (Irp1/2$^{f/f}$) (*Figure 2B*). Irp1 and Irp2 protein expression was markedly reduced in LV myocardium and barely detectable in isolated cardiomyocytes from Cre-Irp1/2$^{f/f}$ mice (*Figure 2C and D*). Irp1 and Irp2 protein expression in the liver was similar in Cre-Irp1/2$^{f/f}$ and Irp1/2$^{f/f}$ mice (*Figure 2C* and *D*). IRE binding activity was strongly reduced in isolated cardiomyocytes from Cre-Irp1/2$^{f/f}$ mice (*Figure 2E*), confirming near-complete Cre-mediated recombination. Iron-regulatory protein/IRE-regulated proteins involved in iron transport and storage were differentially regulated in cardiomyocytes from Cre-Irp1/2$^{f/f}$ mice: the transferrin receptor was down-regulated (25 ± 14% of Irp1/2$^{f/f}$ controls, $P = 0.006$), whereas ferroportin (325 ± 9%, $P = 0.003$) and ferritin H-chain (249 ± 35%, $P = 0.012$) were up-regulated ($n = 3$ per group; representative immunoblots are presented in *Figure 2F*). As a result, iron concentration in cardiomyocytes was significantly reduced in Cre-Irp1/2$^{f/f}$ mice (*Figure 2G*). Likewise, iron concentration in the left ventricle was reduced in Cre-Irp1/2$^{f/f}$ mice compared with Irp1/2$^{f/f}$ controls, whereas iron concentrations in the M. quadriceps femoris and liver were not affected (*Figure 2H*). Iron concentration in the left ventricle was normal in Cre mice showing that cardiac ID in Cre-Irp1/2$^{f/f}$ mice was not related to Cre transgene expression per se (*Figure 2H*). Haem and myoglobin concentrations were significantly reduced in the left ventricle of Cre-Irp1/2$^{f/f}$ mice (*Figure 2I* and *J*). Copper and free radical concentrations in the left ventricle were similar in Cre-Irp1/2$^{f/f}$ and Irp1/2$^{f/f}$ mice (see Supplementary material on line, *Figure S2*).

Cre-Irp1/2$^{f/f}$ mice did not show an obvious phenotype under baseline conditions. Body mass, heart mass, LV mass, and cardiomyocyte cross-sectional area were similar in Cre-Irp1/2$^{f/f}$ and Irp1/2$^{f/f}$ mice under baseline conditions (see Supplementary material online, *Table S1*). On echocardiography, LV end-diastolic and end-systolic dimensions and LV systolic and diastolic function were similar in both genotypes (see Supplementary material online, *Table S1*). Cre-Irp1/2$^{f/f}$ mice were not anaemic and had a normal peripheral blood count (see Supplementary material online, *Table S2*).

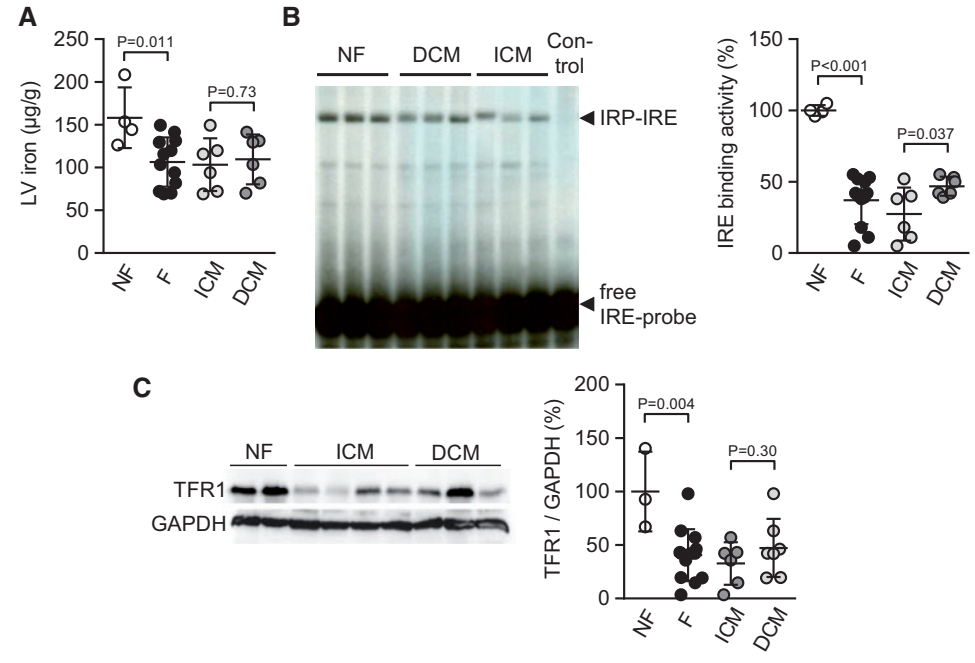

Figure 1 *Reduced IRP activity and iron content in failing human hearts.* (*A*) Non-haem iron concentration in left ventricular (LV) tissue samples from non-failing donors (NF) and patients with cardiac failure (*F*) due to ischemic cardiomyopathy (ICM) or dilated cardiomyopathy (DCM); $n = 4$–6 per group. (*B*) Representative electrophoretic mobility shift assay and summary data showing iron-responsive element (IRE) binding activity in LV tissue samples; $n = 4$–6 (control, no sample loaded). (*C*) Representative immunoblot and summary data showing transferrin receptor 1 (TFR1) and GAPDH protein expression in LV tissue samples; $n = 3$–7. *P* values were determined by two independent sample *t*-test.

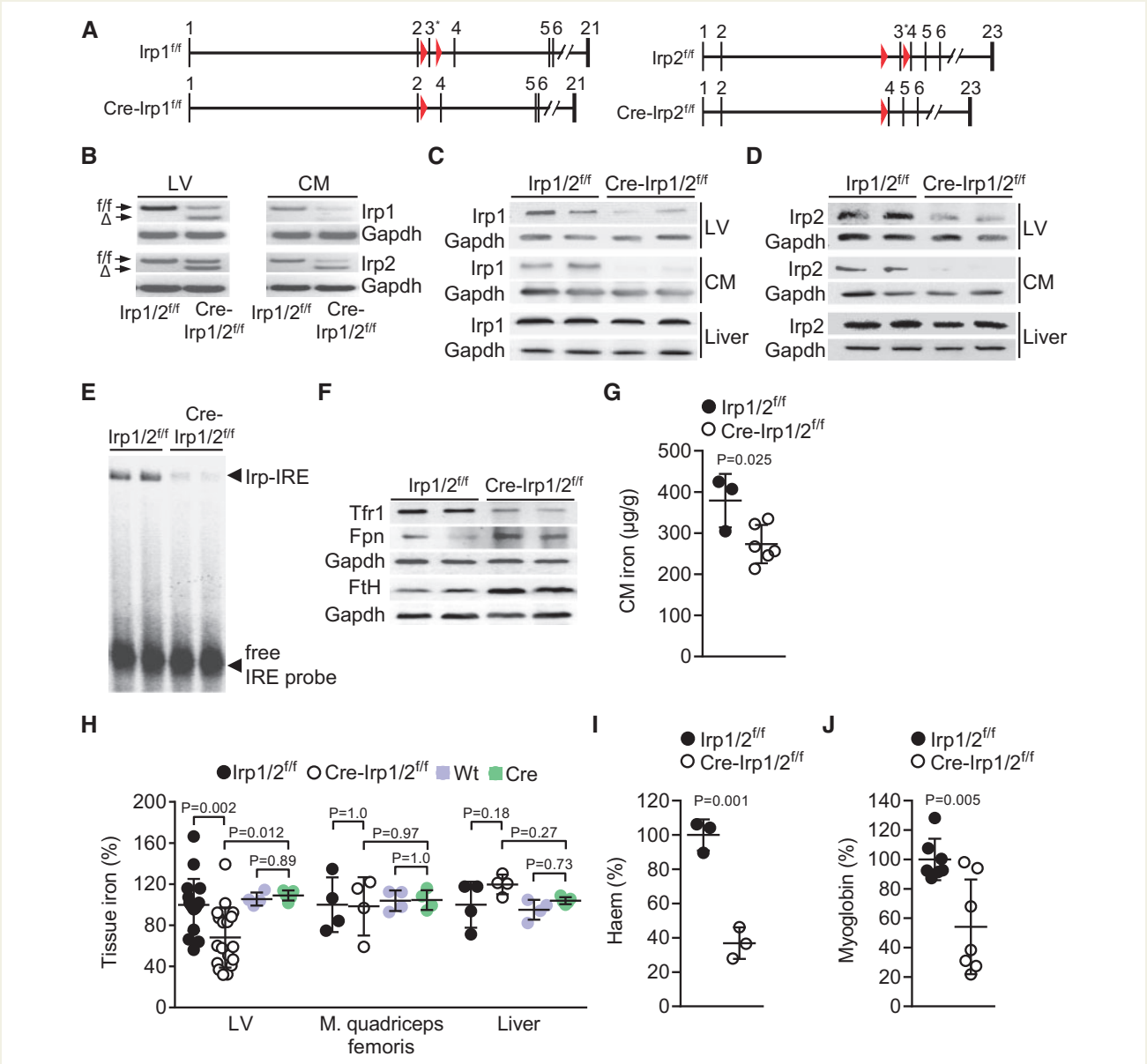

Figure 2 *Mice with targeted Irp deletion develop ID in the myocardium.* (*A*) Cre-LoxP strategy for targeted deletion of exon 3 (indicated by asterisks) in the *Irp1* and *Irp2* genomic loci (triangles represent loxP sites). Intron and exon structures before and after Cre-mediated recombination are shown. (*B*) Reverse transcriptase polymerase chain reaction (RT–PCR) confirming Cre-mediated deletion of exon 3 in Irp1 and Irp2 mRNAs in left ventricular (LV) tissue and isolated cardiomyocytes (CM) from Cre-Irp1/2$^{f/f}$ mice compared with littermates lacking Cre (Irp1/2$^{f/f}$); DNA fragments corresponding to the floxed (f/f) or truncated (Δ) mRNAs are detected. (*C*) Irp1 and (*D*) Irp2 protein expression in left ventricle, CM, and liver (immunoblots; Gapdh used as control). (*E*) Representative electrophoretic mobility shift assay showing iron-responsive element (IRE) binding activity in CM. (*F*) Representative immunoblots showing transferrin receptor 1 (Tfr1), ferroportin (Fpn), ferritin H (FtH), and Gapdh protein expression in CM. (*G*) Iron concentration in CM from 3 Irp1/2$^{f/f}$ and 6 Cre-Irp1/2$^{f/f}$ mice. (*H*) Non-haem iron concentration in left ventricle, M. quadriceps femoris, and liver; $n = 4$–19. (*I*) LV haem and (*J*) myoglobin concentration; $n = 3$–7. *P* values were determined by two independent sample *t*-test (*G*, *I*, *J*) or one-way analysis of variance with Tukey's multiple comparison *post hoc* test (*H*).

Irp-targeted mice lack inotropic reserve

Next, we challenged Cre-Irp1/2$^{f/f}$ mice with dobutamine to expose any functional abnormalities under acute hemodynamic stress. Pressure–volume measurements under resting conditions (before initiating dobutamine) revealed no significant differences between Cre-Irp1/2$^{f/f}$ and Irp1/2$^{f/f}$ mice in heart rate, LV end-diastolic and end-systolic volumes and pressures, and LV systolic and diastolic function (*Figure 3A–F*; see Supplementary material online, *Figure S3*). With increasing dobutamine doses, heart rate increased to a similar extent in Cre-Irp1/2$^{f/f}$ and Irp1/2$^{f/f}$ mice (*Figure 3C*). Systolic function, however,

increased in response to dobutamine in Irp1/2$^{f/f}$ mice but failed to increase in Cre-Irp1/2$^{f/f}$ mice (dP/dt_{max}, stroke volume, and stroke work are shown in *Figure 3D–F*; other variables are presented in Supplementary material online, *Figure S3*). In an additional set of animals, we measured load-independent parameters of systolic (end-systolic elastance, dP/dt_{max}-end diastolic volume relationship, and preload recruitable stroke work) and diastolic function (end-diastolic pressure–volume relationship). Under resting conditions, no significant differences between Cre-Irp1/2$^{f/f}$ and Irp1/2$^{f/f}$ mice were observed. During dobutamine infusion, the systolic parameters, but not the diastolic parameter, were significantly reduced in Cre-Irp1/2$^{f/f}$ mice (see Supplementary material online, *Figure S4*).

Pressure–volume measurements revealed no significant differences between Irp1/2$^{f/f}$, Cre, and wild-type mice at baseline and during dobutamine infusions (see Supplementary material online, *Figure S5*). Thus, Irps in cardiomyocytes are necessary to increase contractile performance during inotropic stimulation.

Targeted Irp deletion increases the risk of heart failure after MI

We induced MI in Cre-Irp1/2$^{f/f}$ mice to study the impact of cardiac ID during a chronic increase in myocardial workload. Inflammatory cell accumulation in the infarcted area at 2 and 6 days after MI was similar in Cre-Irp1/2$^{f/f}$ and Irp1/2$^{f/f}$ mice (see Supplementary material online,

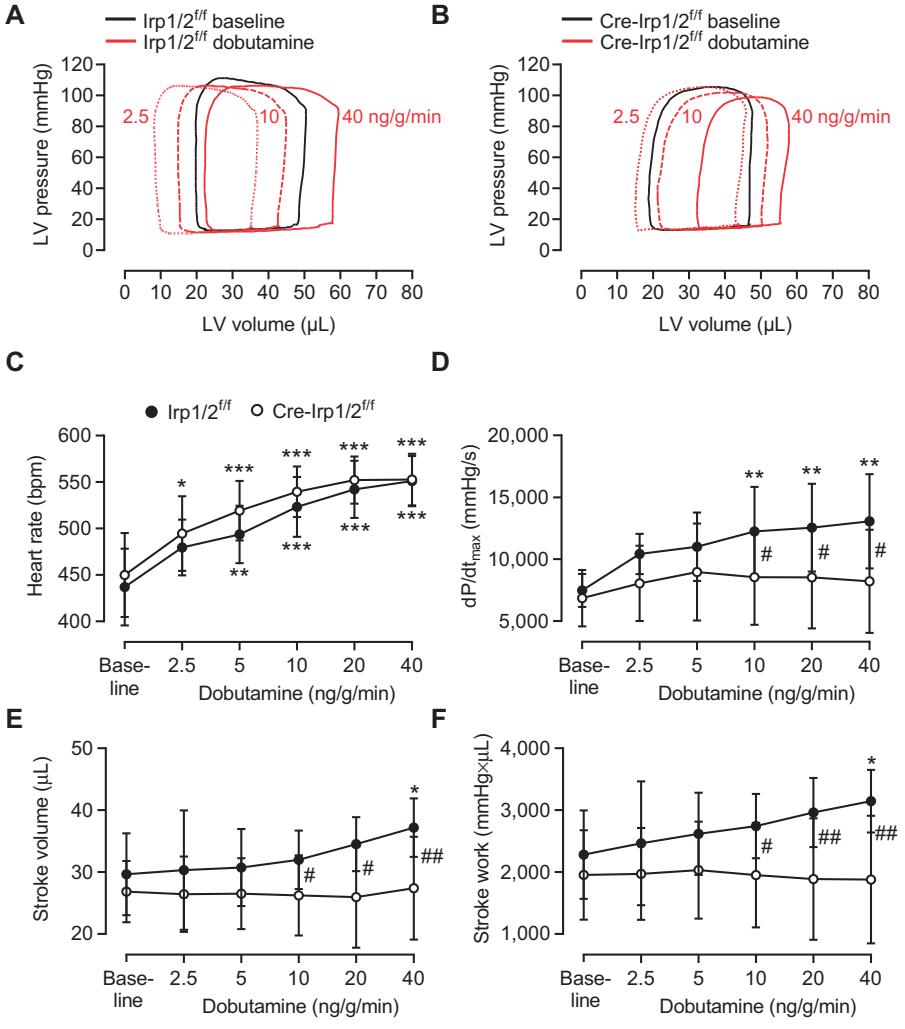

Figure 3 *Mice with targeted Irp deletion lack inotropic reserve.* (*A*) Representative pressure–volume loops from an Irp1/2$^{f/f}$ mouse and (*B*) a Cre-Irp1/2$^{f/f}$ mouse at baseline and during dobutamine infusion (2.5–40 µg/kg body mass per min; 3 min per dose). (*C*) Heart rate, (*D*) dP/dt_{max}, (*E*) stroke volume, and (*F*) stroke work in 9 Irp1/2$^{f/f}$ and 11 Cre-Irp1/2$^{f/f}$ mice (5 Irp1/2$^{f/f}$ and 8 Cre-Irp1/2$^{f/f}$ mice at the lowest dobutamine dose). $^{*}P < 0.05$, $^{**}P < 0.01$, $^{***}P < 0.001$ vs. same genotype at baseline (one-way analysis of variance with Dunnett's multiple comparison *post hoc* test); $^{\#}P < 0.05$, $^{\#\#}P < 0.01$ Cre-Irp1/2$^{f/f}$ vs. Irp1/2$^{f/f}$ (two independent sample *t*-test).

Figure S6). Infarct scar size (*Figure 4A*) and interstitial fibrosis in the non-infarcted left ventricle (see Supplementary material online, *Figure S6*) were similar in Cre-Irp1/2$^{f/f}$ and Irp1/2$^{f/f}$ mice at 28 days after MI. Cre-Irp1/2$^{f/f}$ mice, however, developed more pronounced LV hypertrophy (*Figure 4B*) with greater increases in cardiomyocyte size on histological and single cell examination (*Figure 4C* and *D*), and more pronounced expression of embryonic marker genes (see Supplementary material online, *Figure S7*). Enhanced hypertrophy in Cre-Irp1/2$^{f/f}$ mice was associated with higher expression of the calcineurin-NFAT target gene Rcan1 (*Figure 4E*). Other hypertrophic signalling pathways (Erk1/2, p38-Mapk, and Akt) were not differentially activated after MI in Cre-Irp1/2$^{f/f}$ and Irp1/2$^{f/f}$ mice (see Supplementary material online, *Figure S8*). Left ventricular dilatation and systolic dysfunction after MI were more pronounced in Cre-Irp1/2$^{f/f}$ mice than in Irp1/2$^{f/f}$, Cre, and wild-type control mice (*Figure 4F*). Cre-Irp1/2$^{f/f}$ mice developed overt HF as evidenced by pulmonary congestion (greater lung mass to body mass ratio in *Figure 4G*) and increased mortality (*Figure 4H*). On autopsy, serous fluid accumulation in the chest cavity, indicative of HF, was found in the majority of Cre-Irp1/2$^{f/f}$ mice; we observed only few cardiac ruptures (*Figure 4I*). Thus, Irps in cardiomyocytes protect against HF after MI.

Targeted Irp deletion impairs mitochondrial respiration and cardiac energetics

Considering the importance of iron for mitochondrial energy production, we examined mitochondrial structure and respiratory function in Cre-Irp1/2$^{f/f}$ hearts. We first assessed mitochondrial structural integrity by electron microscopy. Mitochondria were well aligned between the longitudinally oriented myofibrils in Cre-Irp1/2$^{f/f}$ and Irp1/2$^{f/f}$ mice (*Figure 5A*). Mitochondrial density and organization of the cristae appeared normal in Cre-Irp1/2$^{f/f}$ cardiomyocytes (*Figure 5A*). Mitochondrial DNA copy number in the LV myocardium was not significantly altered in Cre-Irp1/2$^{f/f}$ mice (*Figure 5B*), as was the activity of several Krebs cycle enzymes, not containing haem or iron–sulphur clusters (*Figure 5C*). Expression levels of mitochondrial ferritin and ATP-binding cassette transporter 7 were increased, whereas frataxin expression was unchanged in Cre-Irp1/2$^{f/f}$ cardiomyocytes (see Supplementary material online, *Figure S9*).

Although these observations suggested that mitochondrial structure and metabolic function are preserved in Cre-Irp1/2$^{f/f}$ hearts, the activity of the Fe-S cluster-containing complex I of the mitochondrial electron transport chain was markedly lower in left ventricles from Cre-Irp1/2$^{f/f}$ mice (*Figure 5D*). Notably, the activity of haem-containing complex IV was not affected (*Figure 5D*). To directly assess mitochondrial respiration, we measured OCR in isolated cardiomyocytes (*Figure 5E*). Under baseline conditions, OCR was not significantly different between Cre-Irp1/2$^{f/f}$ and Irp1/2$^{f/f}$ cardiomyocytes. Upon addition of the ATP synthase inhibitor oligomycin, OCR dropped to a similar extent in Cre-Irp1/2$^{f/f}$ and Irp1/2$^{f/f}$ cardiomyocytes, indicating that ATP production rate at baseline and proton leak were comparable in both genotypes. To determine maximal respiration, we added carbonyl cyanide 4-(trifluoromethoxy) phenylhydrazone (FCCP), a potent uncoupler of oxidative phosphorylation in mitochondria. The FCCP-stimulated increase in OCR was severely blunted in Cre-Irp1/2$^{f/f}$ cardiomyocytes (*Figure 5E*). Accordingly, spare respiratory capacity was diminished in Cre-Irp1/2$^{f/f}$ cardiomyocytes (130 ± 83% vs. 39 ± 85% increase in OCR over baseline in Cre-Irp1/2$^{f/f}$ and Irp1/2$^{f/f}$ cardiomyocytes, respectively; $P = 0.002$). We finally added the electron transport chain inhibitors antimycin A and rotenone to assess non-mitochondrial respiration and found that OCR dropped to very low levels that were similar in Cre-Irp1/2$^{f/f}$ and Irp1/2$^{f/f}$ cardiomyocytes (*Figure 5E*). Along with OCR we assessed ECAR, which provides a measure of glycolytic activity (lactic acid production) (*Figure 5F*). At baseline, ECAR was not significantly different between Cre-Irp1/2$^{f/f}$ and Irp1/2$^{f/f}$ cardiomyocytes. After addition of FCCP and collapse of the mitochondrial membrane potential, ECAR increased in Irp1/2$^{f/f}$ and, to a smaller extent, in Cre-Irp1/2$^{f/f}$ cardiomyocytes as the cells attempted to maintain energy production by glycolysis (*Figure 5F*). Next, we treated cardiomyocytes with dobutamine to measure mitochondrial respiration during submaximal, physiological stress. Oxygen consumption rate increased in response to dobutamine in Irp1/2$^{f/f}$ cardiomyocytes but not in Cre-Irp1/2$^{f/f}$ cardiomyocytes (*Figure 5G*). Finally, we employed ^{31}P-magnetic resonance spectroscopy at high spatial resolution to study cardiac energy metabolism *in vivo* (*Figure 5H*). Under baseline conditions, PCr/ATP ratio in the left ventricle was similar in Cre-Irp1/2$^{f/f}$ and Irp1/2$^{f/f}$ mice. During dobutamine stress, PCr/ATP ratio remained stable in Irp1/2$^{f/f}$ control mice but dropped significantly in Cre-Irp1/2$^{f/f}$ mice, showing that provision of high energy phosphates is limited in Irp-targeted hearts.

Irp-targeted mice are rescued by intravenous iron supplementation

We examined whether Irp-targeted mice with cardiac ID can be rescued by iron supplementation. A single intravenous injection of ferric carboxymaltose normalized LV myocardial iron concentration in Cre-Irp1/2$^{f/f}$ mice but did not further increase myocardial iron in Irp1/2$^{f/f}$ control mice (*Figure 6A*). Left ventricular myocardial copper and free radical concentrations were not affected by iron supplementation in both genotypes (see Supplementary material online, *Figure S2*). Iron supplementation did not affect OCR under baseline conditions and after maximal stimulation with FCCP in Irp1/2$^{f/f}$ cardiomyocytes (*Figure 6B*). Iron supplementation also did not affect baseline OCR in Cre-Irp1/2$^{f/f}$ cardiomyocytes. Iron supplementation, however, restored maximal OCR (*Figure 6B*) and spare respiratory capacity in FCCP-stimulated Cre-Irp1/2$^{f/f}$ cardiomyocytes (163 ± 192% vs. 55 ± 85% increase in OCR over baseline with or without iron supplementation, respectively; $P = 0.007$). Iron supplementation did not enhance heart rate or systolic function in dobutamine-stimulated Irp1/2$^{f/f}$ mice but restored systolic function in dobutamine-stimulated Cre-Irp1/2$^{f/f}$ mice. Heart rate, dP/dt_{max}, stroke volume, and stroke work during infusion of 40 ng/g/min dobutamine are shown in *Figure 6C–F*; complete dose–response curves of iron supplemented mice are presented in Supplementary material online, *Figure S10*; load-independent parameters are shown in Supplementary material online, *Figure S4*. Enhanced post-infarct cardiomyocyte hypertrophy (*Figure 7A*) and Rcan1 expression (*Figure 7B*) in Cre-Irp1/2$^{f/f}$ mice were prevented by iron supplementation. Iron supplementation also attenuated LV dilatation (*Figure 7C* and *D*) and improved LV systolic function (*Figure 7E*) in Cre-Irp1/2$^{f/f}$ mice. Iron supplementation did

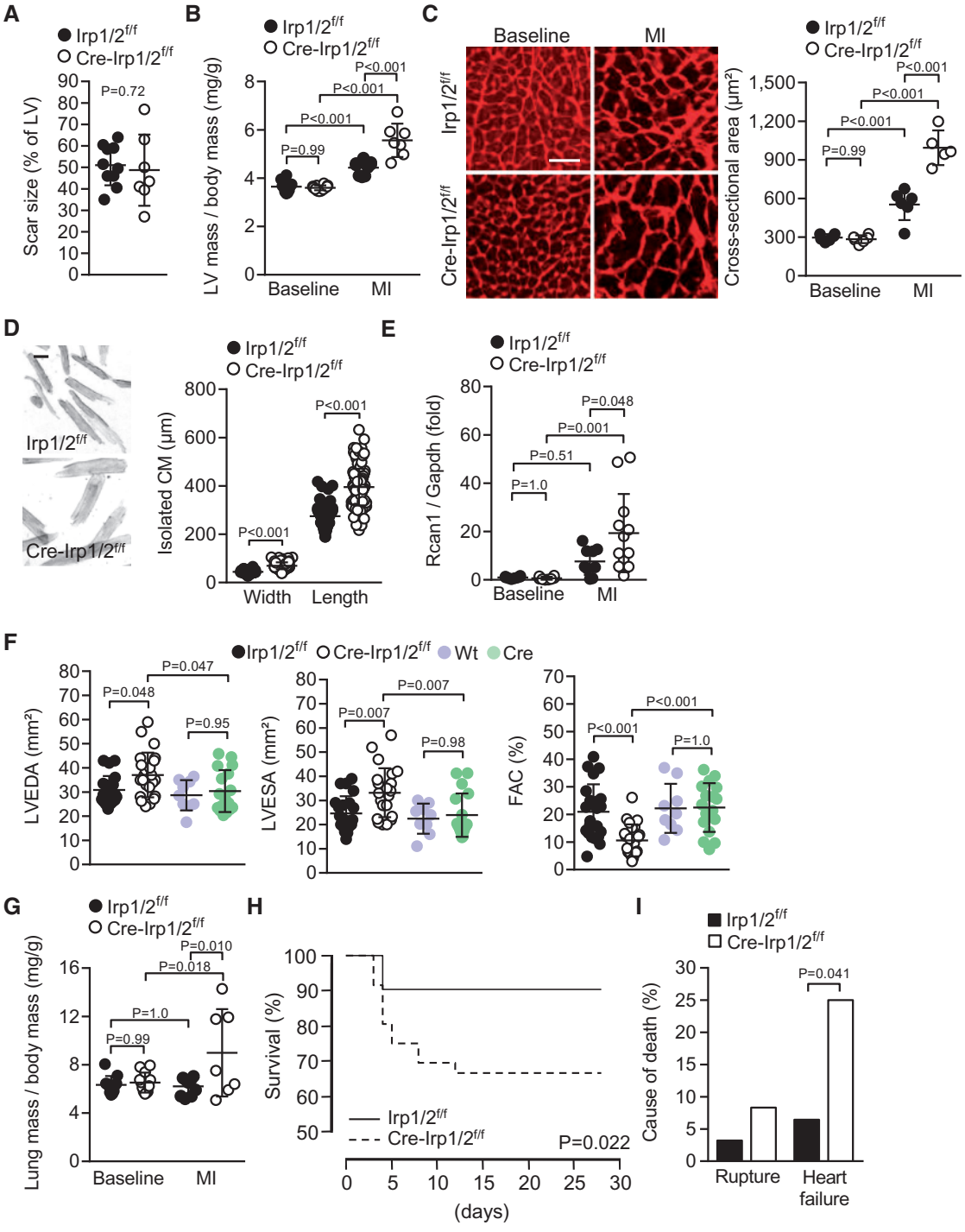

Figure 4 *Targeted Irp deletion promotes heart failure after MI.* (*A*) Infarct scar size in 10 Irp1/2$^{f/f}$ and 7 Cre-Irp1/2$^{f/f}$ mice 28 days after MI. (*B*) Left ventricular (LV) mass to body mass ratio at baseline and 28 days after MI; $n = 7–12$. (*C*) LV cardiomyocyte cross-sectional area at baseline and 28 days after MI; $n = 5–6$. Representative tissue sections stained with wheat germ agglutinin are shown on the left (scale bar, 50 µm). (*D*) Cardiomyocyte (CM) width and length 28 days after MI; 3 mice per group (data points represent individual CM). Representative images are shown on the left (scale bar, 100 µm). (*E*) LV regulator of calcineurin 1 (Rcan1) mRNA expression [reverse transcriptase quantitative polymerase chain reaction (RT–qPCR), normalized to Gapdh] at baseline and 28 days after MI (non-infarcted region); $n = 8–12$. (*F*) LV end-diastolic area, end-systolic area, and fractional area change as determined by echocardiography 28 days after MI; $n = 9–23$. (*G*) Lung mass to body mass ratio at baseline and 28 days after MI; $n = 7–12$. (*H*) Cumulative survival in 31 Irp1/2$^{f/f}$ and 36 Cre-Irp1/2$^{f/f}$ mice after MI. (*I*) Cause of death (same animals as in panel *H*). *P* values were determined by two independent sample *t*-test (*A*, *D*), two-way analysis of variance with Tukey's multiple comparison *post hoc* test (*B*, *C*, *E*, *F*, *G*), log-rank test (*H*), or χ^2 test (*I*).

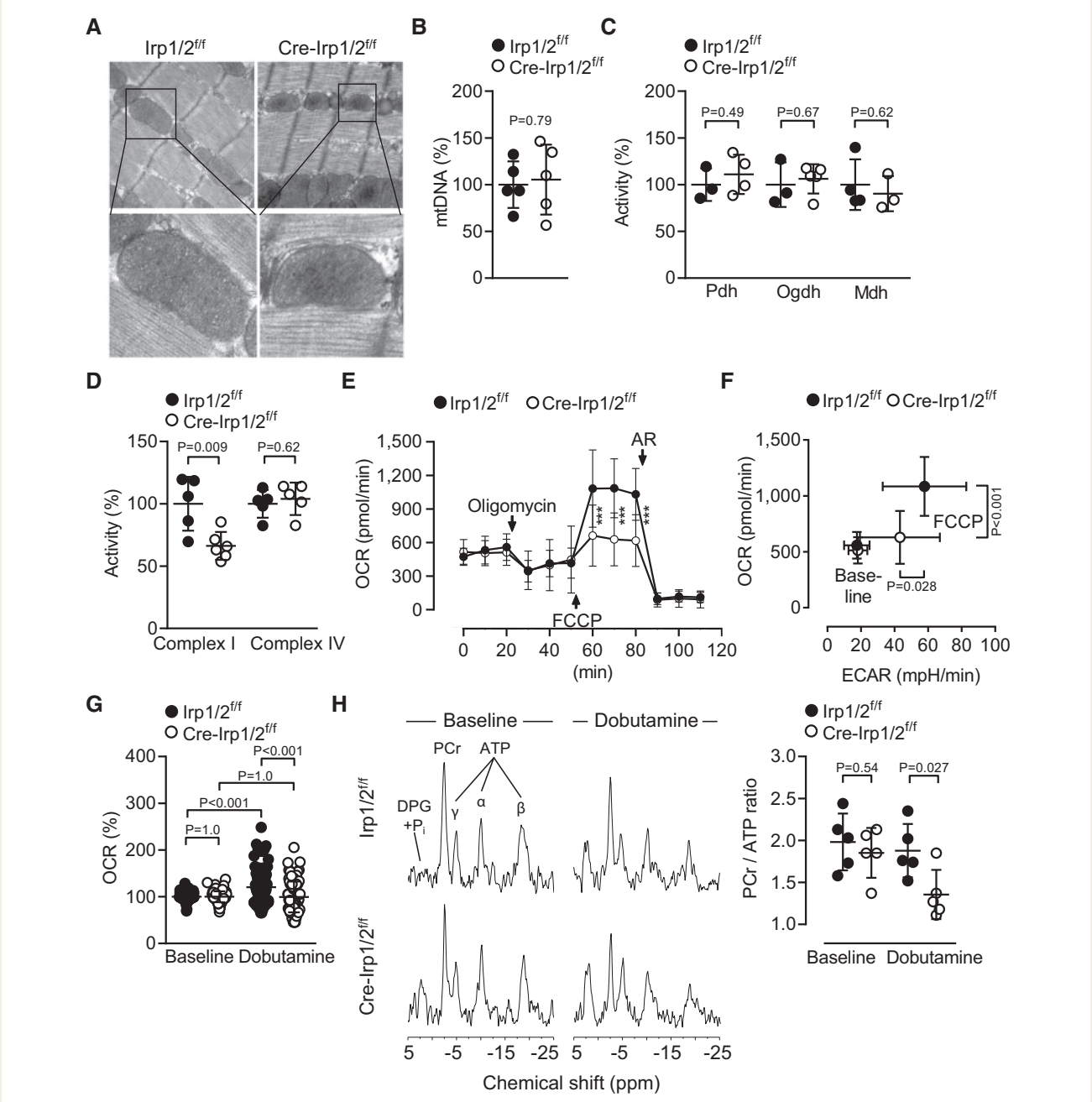

Figure 5 *Impaired mitochondrial respiration and cardiac energetics in Irp-targeted mice.* (*A*) Electron microscopy images showing sarcomeric structure and mitochondrial morphology in left ventricular (LV) tissue sections from Irp1/2$^{f/f}$ and Cre-Irp1/2$^{f/f}$ mice. (*B*) Mitochondrial DNA copy number [quantitative polymerase chain reaction (qPCR) normalized to β-globin] in LV tissue; $n = 5$ per group. (*C*) Activity of the Krebs cycle enzymes pyruvate dehydrogenase (Pdh), oxoglutarate dehydrogenase (Ogdh), and malate dehydrogenase (Mdh) in LV tissue; $n = 3$–5. (*D*) Enzymatic activity of complex I and complex IV of the mitochondrial electron transport chain in LV tissue; $n = 5$–6. (*E*) Oxygen consumption rate (OCR) of isolated Irp1/2$^{f/f}$ and Cre-Irp1/2$^{f/f}$ cardiomyocytes (CM) under baseline conditions and after consecutive addition of oligomycin, carbonyl cyanide 4-(trifluoromethoxy)phenylhydrazone (FCCP), and antimycin A plus rotenone (AR); $n = 3$ experiments; ***$P < 0.001$ Cre-Irp1/2$^{f/f}$ vs. Irp1/2$^{f/f}$. (*F*) OCR and extracellular acidification rate (ECAR) under baseline conditions and after addition of FCCP (same experiments as in panel *E*). (*G*) OCR of isolated Irp1/2$^{f/f}$ and Cre-Irp1/2$^{f/f}$ CM under baseline conditions and during dobutamine stimulation (2.5 µmol/L); $n = 3$ experiments (data points represent individual CM wells). (*H*) Representative ^{31}P-magnetic resonance spectra and PCr/ATP ratios in the LV free wall at baseline and during dobutamine infusion (40 ng/g/min); $n = 5$. *P* values were determined by two independent sample *t*-test (*B*, *C*, *D*, *E*, *H*) or two-way analysis of variance with Tukey's multiple comparison *post hoc* test (*F*, *G*).

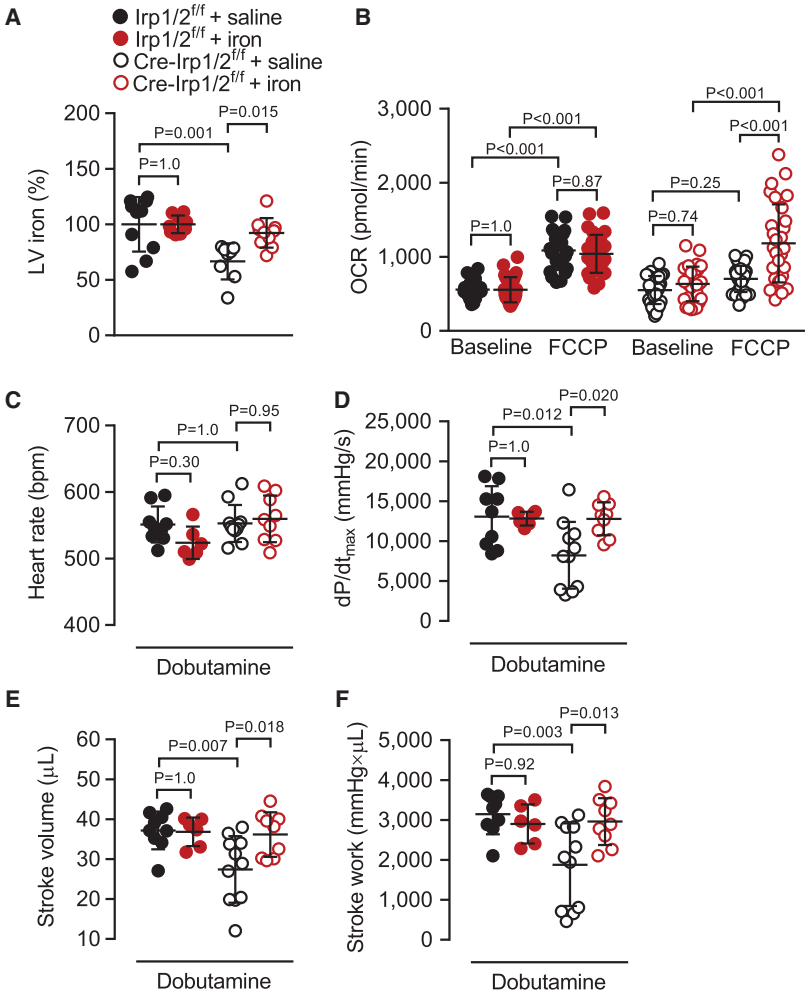

Figure 6 *Iron supplementation rescues mitochondrial respiration and inotropic reserve in Irp-targeted mice.* Irp1/2$^{f/f}$ and Cre-Irp1/2$^{f/f}$ mice were treated with a single intravenous injection of ferric carboxymaltose (20 µg/g body mass) or saline 5 days before the experiments. (*A*) Left ventricular (LV) non-haem iron concentration; $n = 8$–10 per group. (*B*) Oxygen consumption rate (OCR) of isolated cardiomyocytes (CM) under baseline conditions and after stimulation with carbonyl cyanide 4-(trifluoromethoxy)phenylhydrazone (FCCP); $n = 3$ experiments (data points represent individual CM wells). (*C*) Heart rate, (*D*) dP/dt_{max}, (*E*) stroke volume, and (*F*) stroke work during dobutamine stimulation (40 ng/g/min); $n = 6$–11. *P* values were determined by two-way analysis of variance with Tukey's multiple comparison *post hoc* test.

not have an impact on LV cardiomyocyte hypertrophy, remodelling, and systolic function in Irp1/2$^{f/f}$ mice (*Figure 7A–E*).

Mice with a cardiomyocyte-targeted deletion of Irp1 or Irp2 have no cardiac phenotype

To assess whether the two Irps are functionally redundant, we generated mice with a cardiomyocyte-targeted deletion of *Irp1* (Cre-Irp1$^{f/f}$) or *Irp2* (Cre-Irp2$^{f/f}$). Iron concentrations in the left ventricle were not reduced in single Irp mutant mice compared with the floxed controls lacking the Cre transgene (Irp1$^{f/f}$ and Irp2$^{f/f}$). Pressure–volume measurements under resting conditions and during dobutamine infusions revealed no significant differences between single Irp mutant and control mice. Left ventricular cardiomyocyte hypertrophy, LV end-diastolic and end-systolic dimensions, and systolic function were not significantly different between single Irp mutant and control mice (see Supplementary material online, *Figure S11*).

Discussion

Iron deficiency is associated with adverse outcomes in HF, and it has been speculated that iron depletion in the myocardium contributes to systolic dysfunction and disease progression.[1] Because ID and anaemia are inextricably linked, dissecting out the functional importance of ID vs. anaemia has proved extremely difficult. Here, we define the pathophysiological role of IRPs and iron in the heart (*Figure 8*).

Using Cre-loxP technology, we generated mice with targeted deletion of *Irp1* and *Irp2* in cardiomyocytes. The transferrin receptor was down-regulated, whereas ferroportin and ferritin were up-regulated in Irp-targeted cardiomyocytes. Reflecting net changes in iron import,

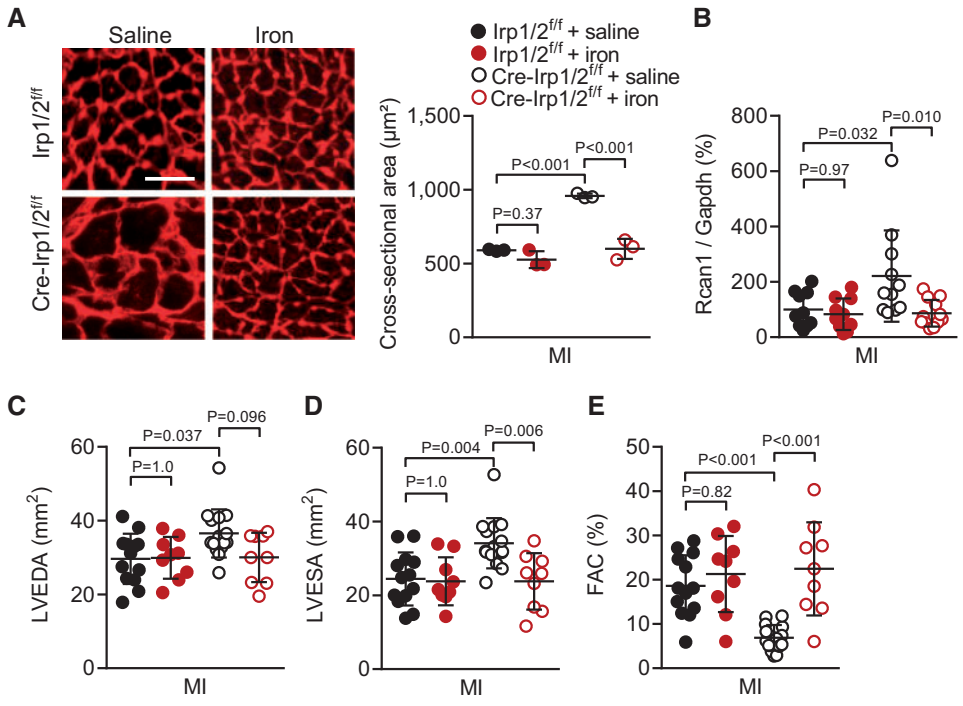

Figure 7 *Iron supplementation attenuates maladaptive LV remodelling in Irp-targeted mice.* Irp1/2$^{f/f}$ and Cre-Irp1/2$^{f/f}$ mice were treated with a single intravenous injection of ferric carboxymaltose (20 µg/g body mass) or saline 5 days before coronary artery ligation (MI). (*A*) Left ventricular (LV) cardiomyocyte cross-sectional area 14 days after MI; $n = 3$ per group. Representative tissue sections stained with wheat germ agglutinin are shown on the left (scale bar, 50 µm). (*B*) Regulator of calcineurin 1 (Rcan1) mRNA expression [reverse transcriptase polymerase chain reaction (RT–qPCR), normalized to Gapdh] in the non-infarcted region of the left ventricle 14 days after MI; $n = 9$–11. (*C*) LV end-diastolic area, (*D*) end-systolic area, and (*E*) fractional area change as determined by echocardiography 14 days after MI; $n = 9$–15. *P* values were determined by two-way analysis of variance with Tukey's multiple comparison *post hoc* test.

export, and sequestration, iron concentration was reduced in Irp-targeted cardiomyocytes. Mice with a targeted deletion of only one Irp isoform did not develop cardiac ID and displayed no cardiac phenotype. We conclude that the two Irps redundantly secure iron availability in cardiomyocytes, like in other cell types,[14–16] by modulating the expression of canonical iron metabolism genes. Importantly, Irp-targeted mice were not anaemic and had preserved tissue iron levels outside the heart, thus enabling us to study the effects of cardiac ID without the confounding influence of systemic ID and anaemia.

Iron concentration in the left ventricle was reduced by 32% in Irp-targeted mice, a reduction that is similar in magnitude to what we and others have observed in patients with heart failure.[5,6] The mechanisms leading to ID in the failing human heart are not well understood but may be related to reduced systemic iron availability.[2,3] We show for the first time that IRP activity in the heart is diminished in patients with ischemic or dilated cardiomyopathy and cardiac ID. Low IRP activity was associated with reduced transferrin receptor expression levels in our patients. Considering that IRPs enhance transferrin receptor expression by post-transcriptional mechanisms[13] and that transferrin receptor expression and iron content were reduced in Irp-targeted cardiomyocytes, we propose that reduced IRP activity and iron uptake contribute to ID in the failing human heart.

Haem biosynthesis depends on iron to metallate protoporphyrin IX, and this process is catalysed by the iron–sulphur cluster-containing enzyme ferrochelatase.[17] Haem concentration in the left ventricle was reduced in Irp-targeted mice. Expression of the haem protein myoglobin was reduced as well, but the activity of the haem-containing complex IV of the mitochondrial electron transport chain was preserved. Conversely, the activity of the Fe-S cluster-containing complex I was reduced, indicating that iron-deficient hearts prioritized their use of iron and haem. Mitochondria need iron to fuel haem and iron–sulphur cluster biosynthetic pathways, but iron is also required for mitochondrial biogenesis and to preserve mitochondrial structure.[18,19] Iron deprivation may result in a decrease in mitochondrial protein abundance that affects both iron-containing and non-iron-containing proteins.[18] Accordingly, mitochondrial structure is severely disrupted in mice with a cardiomyocyte-targeted deletion of the transferrin receptor, and these animals die within 2 weeks after birth.[19] Irp-targeted mice that still expressed the transferrin receptor in cardiomyocytes (albeit at reduced levels), and which developed cardiac ID (but not complete iron deprivation), displayed a milder phenotype. Mitochondrial structure was preserved in these animals. The activity of Krebs cycle enzymes, not containing haem or iron–sulphur clusters, was normal, thus excluding a general disruption of mitochondrial metabolic function. Moreover, mitochondrial respiration and heart function under resting conditions were preserved in Irp-targeted mice, indicating a remarkable resistance of the heart to ID. Similarly, ID is most often not associated with overt cardiac disease in

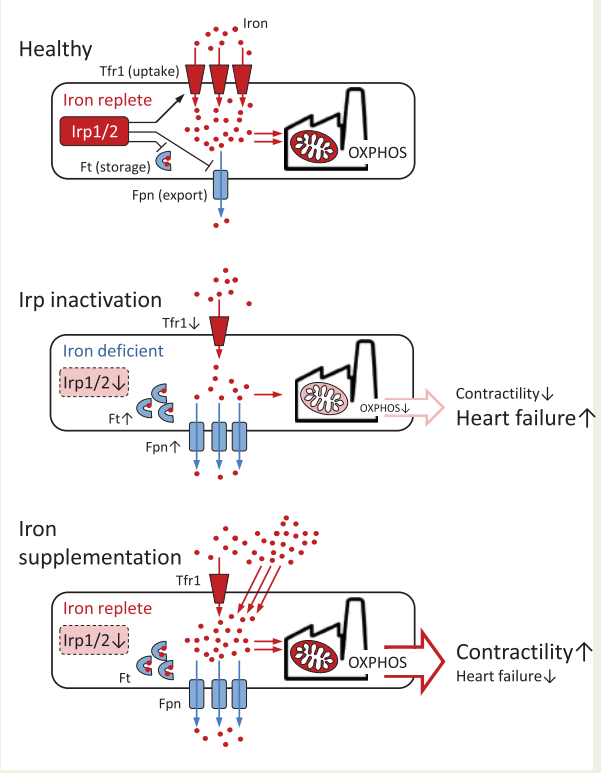

Figure 8 *Summary of key findings.* Iron-regulatory proteins (Irp1/2) secure iron availability in cardiac myocytes by enhancing iron uptake (via the transferrin receptor, Tfr1) and reducing iron export (via ferroportin, Fpn) and storage (bound to ferritin, Ft). Under iron replete conditions, enough iron is available to feed iron–sulphur cluster-containing proteins required for mitochondrial oxidative phosphorylation (OXPHOS). Reflecting net changes in iron uptake, export, and storage, cardiomyocyte-selective Irp inactivation leads to intracellular ID. Similarly, IRP activity is reduced in the failing human heart. Iron deficiency in cardiomyocytes impairs oxidative phosphorylation and adaptation to acute and chronic increases in workload. Iron supplementation restores intracellular iron availability by increasing Tfr1- and non-Tfr1-mediated iron uptake, thereby enhancing oxidative phosphorylation and resistance to stress.

otherwise healthy individuals, especially in the absence of severe anaemia.[20,21]

The energetic requirements of the heart during increases in workload are met by enhanced mitochondrial oxidative phosphorylation and ATP production. To ensure a high level of free energy release from ATP hydrolysis over a wide range of cardiac loads, intracellular ATP is constantly replenished and free ADP concentration is kept low via the creatine kinase reaction. A decreased PCr/ATP ratio is therefore a sensitive indicator of an underlying energetic deficit.[22,23] Consistent with a previous report,[23] the PCr/ATP ratio in the left ventricle remained stable during dobutamine stress in control mice, confirming that provision of high energy phosphates is not a limiting factor in iron replete hearts. In contrast, PCr/ATP ratio dropped significantly in dobutamine-stimulated Irp-targeted mice. Metabolic profiling of isolated cardiomyocytes showed that mitochondrial respiration, while preserved under baseline conditions, increased only slightly upon maximal stimulation with an uncoupling agent and did not increase in response to dobutamine in Irp-targeted mice. Of note, the energetic deficit in Irp-targeted mice was not compensated by enhanced glycolysis. We conclude that Irp-targeted, iron-deficient cardiomyocytes are unable to increase mitochondrial oxidative phosphorylation during inotropic stimulation.

After MI, Irp-targeted mice developed more severe LV remodelling, with more pronounced hypertrophy and systolic dysfunction, and increased HF mortality. Mutations affecting myocardial energy production may result in hypertrophic or dilated cardiomyopathies in patients.[24] More specifically, ~40% of children with inherited complex I deficiencies present with cardiac involvement.[25] Mutations in one of the ~45 protein subunits of complex I have been shown to result in heart failure in mice.[26,27] In one of these studies, a severe reduction of complex I activity (down to ~10% of normal) resulted in a decreased basal rate of mitochondrial ATP production and the spontaneous development of a fatal cardiomyopathy.[26] Mice with a less severe reduction of complex I activity (~25% of normal) were able to maintain heart function under baseline conditions but developed accelerated HF in response to chronic pressure overload,[27] similar to what we have observed in Irp-targeted mice. Reduced complex I activity may therefore be one important mechanism linking cardiac ID to post-infarct HF. Yet, considering the large number of iron-containing mitochondrial, cytosolic, and nuclear proteins that may be affected by cardiac ID,[28,29] e.g. iron-containing enzymes,[30] and secondary gene expression changes (e.g. in mitochondrial ferritin), additional mechanisms may be at play and Irp-targeted mice will be a useful tool to explore them.

Importantly, Irp-targeted mice were rescued by a single intravenous injection of ferric carboxymaltose. Iron supplementation refilled cardiac iron stores, restored mitochondrial respiratory function, and inotropic reserve and attenuated adverse post-infarct remodelling. The therapeutic effects of iron supplementation establish cardiac ID as the leading disease mechanism in Irp-targeted mice. Iron did not enhance baseline heart function in these animals, emphasizing that cardiac iron content, although reduced, is sufficient to maintain heart function under unstressed conditions. Our data also indicate that iron supplementation can replenish depleted cardiac iron stores even when cardiac (myocyte) transferrin receptor expression is low (such as in Irp-targeted myocytes), a situation when non-transferrin-bound iron uptake may become more important.[31] These observations provide strong mechanistic support for ongoing clinical trials examining the role of iron therapy in HF patients with ID.

Supplementary material

Supplementary material is available at *European Heart Journal* online.

Funding

The German Research Foundation (KE 1748/1-1 to T.K. and Excellence Cluster REBIRTH-2 to K.C.W.); the German Heart Research Foundation (F/41/13 to T.K.); the German-Israeli Foundation for Scientific Research and Development (1061-59.2/2008 to T.K. and K.C.W.).

Conflict of interest: none declared.

References

1. von Haehling S, Jankowska EA, van Veldhuisen DJ, Ponikowski P, Anker SD. Iron deficiency and cardiovascular disease. *Nat Rev Cardiol* 2015;**12**:659–669.
2. Jankowska EA, Rozentryt P, Witkowska A, Nowak J, Hartmann O, Ponikowska B, Borodulin-Nadzieja L, Banasiak W, Polonski L, Filippatos G, McMurray JJ, Anker SD, Ponikowski P. Iron deficiency: an ominous sign in patients with systolic chronic heart failure. *Eur Heart J* 2010;**31**:1872–1880.
3. Jankowska EA, Malyszko J, Ardehali H, Koc-Zorawska E, Banasiak W, von Haehling S, Macdougall IC, Weiss G, McMurray JJ, Anker SD, Gheorghiade M, Ponikowski P. Iron status in patients with chronic heart failure. *Eur Heart J* 2013;**34**:827–834.
4. Jankowska EA, Kasztura M, Sokolski M, Bronisz M, Nawrocka S, Oleskowska-Florek W, Zymlinski R, Biegus J, Siwolowski P, Banasiak W, Anker SD, Filippatos G, Cleland JG, Ponikowski P. Iron deficiency defined as depleted iron stores accompanied by unmet cellular iron requirements identifies patients at the highest risk of death after an episode of acute heart failure. *Eur Heart J* 2014;**35**:2468–2476.
5. Maeder MT, Khammy O, dos Remedios C, Kaye DM. Myocardial and systemic iron depletion in heart failure implications for anemia accompanying heart failure. *J Am Coll Cardiol* 2011;**58**:474–480.
6. Leszek P, Sochanowicz B, Szperl M, Kolsut P, Brzoska K, Piotrowski W, Rywik TM, Danko B, Polkowska-Motrenko H, Rozanski JM, Kruszewski M. Myocardial iron homeostasis in advanced chronic heart failure patients. *Int J Cardiol* 2012;**159**:47–52.
7. Carley AN, Taegtmeyer H, Lewandowski ED. Matrix revisited: mechanisms linking energy substrate metabolism to the function of the heart. *Circ Res* 2014;**114**:717–729.
8. Anker SD, Comin Colet J, Filippatos G, Willenheimer R, Dickstein K, Drexler H, Luscher TF, Bart B, Banasiak W, Niegowska J, Kirwan BA, Mori C, von Eisenhart Rothe B, Pocock SJ, Poole-Wilson PA, Ponikowski P, for the FAIR-HF Trial Investigators. Ferric carboxymaltose in patients with heart failure and iron deficiency. *N Engl J Med* 2009;**361**:2436–2448.
9. Ponikowski P, van Veldhuisen DJ, Comin-Colet J, Ertl G, Komajda M, Mareev V, McDonagh T, Parkhomenko A, Tavazzi L, Levesque V, Mori C, Roubert B, Filippatos G, Ruschitzka F, Anker SD; CONFIRM-HF Investigators. Beneficial effects of long-term intravenous iron therapy with ferric carboxymaltose in patients with symptomatic heart failure and iron deficiency. *Eur Heart J* 2015;**36**:657–668.
10. Neffgen JF, Korecky B. Cellular hyperplasia and hypertrophy in cardiomegalies induced by anemia in young and adult rats. *Circ Res* 1972;**30**:104–113.
11. Petering DH, Stemmer KL, Lyman S, Krezoski S, Petering HG. Iron deficiency in growing male rats: a cause of development of cardiomyopathy. *Ann Nutr Metab* 1990;**34**:232–243.
12. Naito Y, Tsujino T, Matsumoto M, Sakoda T, Ohyanagi M, Masuyama T. Adaptive response of the heart to long-term anemia induced by iron deficiency. *Am J Physiol Heart Circ Physiol* 2009;**296**:H585–H593.
13. Hentze MW, Muckenthaler MU, Galy B, Camaschella C. Two to tango: regulation of mammalian iron metabolism. *Cell* 2010;**142**:24–38.
14. Galy B, Ferring-Appel D, Sauer SW, Kaden S, Lyoumi S, Puy H, Kolker S, Grone HJ, Hentze MW. Iron regulatory proteins secure mitochondrial iron sufficiency and function. *Cell Metab* 2010;**12**:194–201.
15. Galy B, Ferring-Appel D, Becker C, Gretz N, Grone HJ, Schumann K, Hentze MW. Iron regulatory proteins control a mucosal block to intestinal iron absorption. *Cell Rep* 2013;**3**:844–857.
16. Nairz M, Ferring-Appel D, Casarrubea D, Sonnweber T, Viatte L, Schroll A, Haschka D, Fang FC, Hentze MW, Weiss G, Galy B. Iron regulatory proteins mediate host resistance to salmonella infection. *Cell Host Microbe* 2015;**18**:254–261.
17. Ajioka RS, Phillips JD, Kushner JP. Biosynthesis of heme in mammals. *Biochim Biophys Acta* 2006;**1763**:723–736.
18. Rensvold JW, Ong SE, Jeevananthan A, Carr SA, Mootha VK, Pagliarini DJ. Complementary RNA and protein profiling identifies iron as a key regulator of mitochondrial biogenesis. *Cell Rep* 2013;**3**:237–245.
19. Xu W, Barrientos T, Mao L, Rockman HA, Sauve AA, Andrews NC. Lethal cardiomyopathy in mice lacking transferrin receptor in the heart. *Cell Rep* 2015;**13**:533–545.
20. Hegde N, Rich MW, Gayomali C. The cardiomyopathy of iron deficiency. *Tex Heart Inst J* 2006;**33**:340–344.
21. Lopez A, Cacoub P, Macdougall IC, Peyrin-Biroulet L. Iron deficiency anaemia. *Lancet* 2016;**387**:907–916.
22. Tian R, Ingwall JS. Energetic basis for reduced contractile reserve in isolated rat hearts. *Am J Physiol* 1996;**270**:H1207–H1216.
23. Naumova AV, Weiss RG, Chacko VP. Regulation of murine myocardial energy metabolism during adrenergic stress studied by in vivo ^{31}P NMR spectroscopy. *Am J Physiol Heart Circ Physiol* 2003;**285**:H1976–H1979.
24. Watkins H, Ashrafian H, Redwood C. Inherited cardiomyopathies. *N Engl J Med* 2011;**364**:1643–1656.
25. Yaplito-Lee J, Weintraub R, Jamsen K, Chow CW, Thorburn DR, Boneh A. Cardiac manifestations in oxidative phosphorylation disorders of childhood. *J Pediatr* 2007;**150**:407–411.
26. Ke BX, Pepe S, Grubb DR, Komen JC, Laskowski A, Rodda FA, Hardman BM, Pitt JJ, Ryan MT, Lazarou M, Koleff J, Cheung MM, Smolich JJ, Thorburn DR. Tissue-specific splicing of an Ndufs6 gene-trap insertion generates a mitochondrial complex I deficiency-specific cardiomyopathy. *Proc Natl Acad Sci U S A* 2012;**109**:6165–6170.
27. Karamanlidis G, Lee CF, Garcia-Menendez L, Kolwicz SC Jr, Suthammarak W, Gong G, Sedensky MM, Morgan PG, Wang W, Tian R. Mitochondrial complex I deficiency increases protein acetylation and accelerates heart failure. *Cell Metab* 2013;**18**:239–250.
28. Reedy CJ, Elvekrog MM, Gibney BR. Development of a heme protein structure-electrochemical function database. *Nucleic Acids Res* 2008;**36**:D307–D313.
29. Rouault TA. Mammalian iron-sulphur proteins: novel insights into biogenesis and function. *Nat Rev Mol Cell Biol* 2015;**16**:45–55.
30. de Visser SP, Kumar D. *Iron-Containing Enzymes: Versatile Catalysts of Hydroxylation Reactions in Nature*. Cambridge: The Royal Society of Chemistry; 2011.
31. Nam H, Wang CY, Zhang L, Zhang W, Hojyo S, Fukada T, Knutson MD. Zip14 and Dmt1 in the liver, pancreas, and heart are differentially regulated by iron deficiency and overload: implications for tissue iron uptake in iron-related disorders. *Haematologica* 2013;**98**:1049–1057.